Available online at www.sciencedirect.com
ScienceDirect
Atmospheric Environment 41 (2007) 1091–1106
ATMOSPHERIC ENVIRONMENT
www.elsevier.com/locate/atmosenv

The evolution of chemical components of aerosols at five monitoring sites of China during dust storms

Ying Wang[a,b,c], Guoshun Zhuang[a,b,c,d,*], Aohan Tang[b], Wenjie Zhang[b], Yele Sun[b,c], Zifa Wang[c], Zhisheng An[a,d]

[a]*Center for Atmospheric Chemistry Study, Department of Environmental Science & Engineering, Fudan University, Shanghai 200433, China*
[b]*Center for Atmospheric Environmental Study, Department of Chemistry, Beijing Normal University, Beijing 100875, China*
[c]*Institute of Atmospheric Physics, Chinese Academy of Science, NZC/LAPC, Beijing 100029, China*
[d]*State key Laboratory of Loess & Quaternary Geology, Institute of Earth Environment, Chinese Academy of Science, Xi'an 710075, China*

Received 15 July 2006; received in revised form 6 September 2006; accepted 6 September 2006

Abstract

Daily $PM_{2.5}$ and TSP and their chemical composition with two dust events (DS1: 9–10 March and DS2: 27–30 March) were simultaneously observed for the period of 9 March–23 April 2004 from a monitoring network over China. Five monitoring sites were performed along the transport pathway of Asian dust storm, located in Northwest, North, East, and Southeast regions of China. The dust and non-dust days exhibited different characteristics with respect to the composition and the meteorological conditions. In non-dust days, particulate pollution was found to be associated with the city economy, and it primarily consisted of the crustal, the secondary, and the carbonaceous material. In the dust episodes, significant increase in the particle concentration with a large part of the secondary components diluted by the crustal components was observed at all the sites. Particles were getting more and more acidic as the episodic dust progressed eastward. Dust particles were suggested to react with SO_2/NO_X/sulfate/nitrate based on the variations of SO_4^{2-}/Ca^{2+} and NO_3^-/Ca^{2+} along the transport pathway, and the formation mechanism of sulfate and nitrate was proved to be different. Positive matrix factorization analysis showed that the sources from the upstream and the transport pathways could account for 49%, 82%, and 28% of PM mass, crust, and secondary aerosol, respectively, and the contribution decreased, as the dust made its way from source area to the coastal regions. Enrichment factors of the species presented significant correlations among different sites in the dust episodes, suggesting the significant impact of those dust emissions on the local environment.

Keywords: Dust storm; Evolution; Source contribution; $PM_{2.5}$; TSP

1. Introduction

Asian dust aerosol is the major mineral aerosol transported from central Asia to the Pacific, even to the western coast of America (Duce et al., 1991; Arimoto et al., 1997). The composition and morphology of the dust particles can be regulated

*Corresponding author. Center for Atmospheric Chemistry Study, Department of Environmental Science & Engineering, Fudan University, Shanghai 200433, China.
Tel.: +86 21 55664579; fax: +86 21 65642080.
E-mail address: gzhuang@fudan.edu.cn (G. Zhuang).

1352-2310/$ - see front matter © 2006 Elsevier Ltd. All rights reserved.
doi:10.1016/j.atmosenv.2006.09.015

by adsorbing gaseous species, surface reactions, and coagulation with other particles during the transport. These processes influence the atmospheric mass cycles associated with trace gases such as SO_2, NO_X, and HCl (Zhang et al., 1994; Dentener et al., 1996; Song and Carmichael, 2001; Zhang and Iwasaka, 2001). The transport and deposition of the dust aerosols to a certain region of the ocean may control the rate of organism production through controlling the wind-generated trace elements as iron, aluminum, etc., then affect the oceanic ecosystem and have influence on the absorption of CO_2 and the cycle of the variety of the trace elements (especially C, S, and N, etc.), and indirectly impact the global climate change (Zhuang et al., 1992). Thus understanding the physical and chemical characteristics of Asian dust particles during the long-range transport is important in determining their effects on the geochemical cycle and the radiative forcing over this region.

Most studies compared the different physical and chemical features of aerosols during dust and non-dust days at a certain site, such as Beijing (Zhuang et al., 2001; Wang et al., 2005b), Qingdao (Zhang et al., 2003; Guo et al., 2004a, b), Taiwan (Chen et al., 2004; Lee et al., 2006), and Hong Kong (Fang et al., 1999; Cao et al., 2003) in China, Incheon, Ulsan, and Gosan in Korea (Lee et al., 2004; Park et al., 2003), and Kyoto in Japan (Ma et al., 2001). These studies could shed light on the impact of dust storm on the local environment; however, it has been difficult to deduce the change of the aerosol particle features during the transport from the limited monitoring sites. Scarce studies have been done to illustrate the evolution and modification mechanism of dust aerosols from source areas in China to downwind areas in Korea (Yong-Seung et al., 2005) and Japan (Iwasaka et al., 1988; Zhou et al., 1996; Fan et al., 1996; Mori et al., 2003; Trochkine et al., 2003). For example, the change in composition of mineral aerosol particles during the long-range transport of Asian dust-storm and the internally mixing of a large fraction of the mineral aerosol particles with sea salt in Nagasaki were observed by collecting aerosol samples at Hohhot and Beijing in China, and Nagasaki in Japan (Fan et al., 1996). Similarly, the change in size distribution and chemical composition was studied at eight locations in China and Japan along the route of the dust event, and significant amounts of nitrate was found to be associated with dust aerosols during the transport (Mori et al., 2003). Most of the studies focused on the regions in the line of Northern China–Korea–Japan. However, dust can also be transported from central Asia to South China by a strong continental high (Lee et al., 2006). So far there is no report on the effects of dust events on the air quality concurrently in the cities, including those in the southern China, nor mention the variation mechanism of dust aerosol during its transport from north/west China to south/east China. In this study, five monitoring sites were performed along the transport pathway of Asian dust storm, located in Northwest, North, East, and Southeast regions of China in the spring 2004, during which two dust events in the periods of 9–10 March and 27–30 March were observed by most ground-based stations and satellite. This would provide a precious opportunity to study the impact of dust events on the air quality in cities with different distance to the source area, and to illustrate the evolution of dust aerosol along the transport, putting emphasis on the interaction of mineral aerosol with pollution aerosol or acidic gases. Results from this work would offer the basic data for evaluating the effects of dust pollution on the global climate and biogeochemical cycle.

2. Experimental

2.1. Sampling

A $PM_{2.5}$ and TSP monitoring network, with 10 samplers collecting 24-h average samples, was operated in five sites along the pathway of dust storm across China, from 9 March to 23 April 2004. Totally 409 aerosol samples were collected on Whatman® 41 filters (Whatman Inc., Maidstone, UK) by medium-volume samplers (model: (TSP/PM_{10}/$PM_{2.5}$)-2, flow rate: 77.59 L min^{-1}). Intensive sampling was performed during two dust episodes on 9–10 March (DS1) and 27–30 March (DS2). The study region was approximately 1350 km north-to-south and 970 km west-to-east, including two sites near the dust source area (Duolun (DL) and Yulin (YL)), one inland site (Beijing (BJ)) and two coastal sites (Qingdao (QD) in the north and Shanghai (SH) in the south) on the pathway of the dust storm. The locations of those five sites and the source regions of the two dust episodes identified by MODIS are shown in Fig. 1. The detail information on the five sites is presented in Table 1. The samples were put in polyethylene plastic bags right after sampling and reserved in a refrigerator. All those filters were

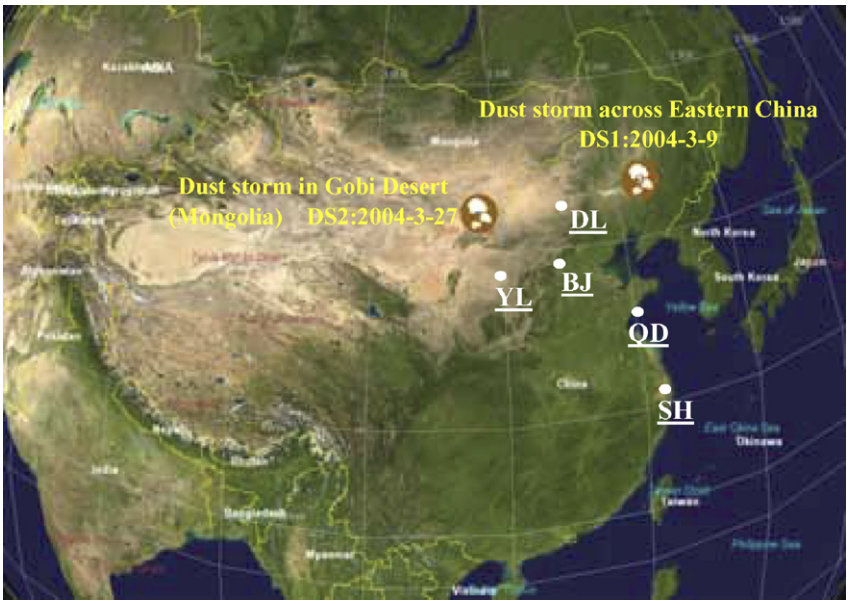

Fig. 1. Map of China indicating the locations of five sampling sites, and the source areas of the two dust episodes identified by MODIS (http://rapidfire.sci.gsfc.gov/).

Table 1
Information on the five sampling sites

Site	Site code	Location coordinates	Area (km^2)	Population (10,000)	GDP (million)	Description
Duolun	DL	42.3N, 116.5E	3773	10.05	521	Inland suburban site: residential regions, sand land
Yulin	YL	38.2N, 109.8E	43,578	329.56	11,136	Inland suburban site: residential and traffic regions, sand land
Beijing	BJ	39.9N, 116.4E	16,800	1136.3	321,271	Inland urban site: residential and traffic regions
Qingdao	QD	36.0N, 120.3E	10,922	715.68	151,817	Coastal urban site: residential and traffic regions
Shanghai	SH	31.2N, 121.5E	6341	1334.23	540,876	Coastal urban site: residential and traffic regions

Data from (China City Statistical Yearbook 2003) for YL, BJ, QD, and SH; from (Inner Mongolia Statistical Yearbook 2004) for DL. All the data are the annual mean values in 2002.

weighed before and after sampling with an analytical balance (Sartorius 2004MP, reading precision 10 μg) after stabilizing under constant temperature ($20\pm1\,^{\circ}C$) and humidity ($40\pm1\%$) for over 24 h. The differences of the mass before and after sampling were divided by the collected sampling volumes to obtain the corresponding concentrations. The meteorological data, including atmospheric pressure, temperature (Temp.), relative humidity (RH), wind speed, wind direction, etc., was downloaded from http://cdc.cma.gov.cn. Mixing depth and sunflux data was collected from http://www.arl.noaa.gov. The average values of these variables during different periods are shown in Table 2.

2.2. Chemical analysis

2.2.1. Ion analysis

One-fourth of each sample and blank filter was extracted ultrasonically by 10 mL water, which was deionized to resistivity of $18\,M\Omega\,cm^{-1}$. After

Table 2
The average values of meteorological variables during the study period

	Pressure (kPa)	Temp. (°C)	RH (%)	Cloud (grade)[a]	Mixdepth (m)	Sunflux ($W m^{-2}$)	Wind speed ($m s^{-1}$)
DS1	95.7	8.3	31.9	5.1	346.9	234.4	5.8
DS2	92.8	8.6	21.9	3.8	427.2	298.7	5.7
ND	95.8	9.9	40.5	4.0	314.0	294.6	3.3

[a]*Note*: grade 0—no cloud; grade 10—total cloud. Data from http://cdc/cma.gov.cn and http://www.arl.noaa.gov.

passing through microporous membranes (pore size, 0.45 μm; diameter, 25 mm; made by the affiliated plant of Beijing chemical school), the filtrates were determined for pH with a pH meter (model, Orion 818). Each filtrate was stored at 4 °C in a clean tube for analysis. 10 anions (SO_4^{2-}, NO_3^-, Cl^-, F^-, PO_4^{3-}, NO_2^-, CH_3COO^-, $HCOO^-$, MSA, $C_2O_4^{2-}$) and five cations (NH_4^+, Ca^{2+}, K^+, Mg^{2+}, Na^+) were analyzed by ion chromatography (IC, model, Dionex 600), which consists of a separation column (Dionex Ionpac AS11 for anion and CS12A for cation), a guard column (Dionex Ionpac AG 11 for anion and AG12A for cation), a self-regenerating suppressed conductivity detector (Dionex Ionpac ED50), and a gradient pump (Dionex Ionpac GP50). The gradient weak base eluent (76.2 mM $NaOH + H_2O$) was used for anion detection, while the weak acid eluent (20 mM MSA) for cation detection. The recovery of each ion was in the range of 80–120%. The relative standard deviation of each ion was less than 5% for reproducibility test. The limits of detection ($S/N = 3$) were less than 0.04 mg L^{-1} for anions and 0.006 mg L^{-1} for cations. The quality assurance was routinely carried out by using standard reference materials (GBW 08606) produced by National Research Center for Certified Reference Materials, China. Blank values were subtracted from sample determinations. The details were given elsewhere (Yuan et al., 2003).

2.2.2. Element analysis

One half of the sample filters were digested at 170 °C for 4 h in high-pressure Teflon digestion vessel with 3 mL concentrated HNO_3, 1 mL concentrated HCl, and 1 mL concentrated HF. After cooling, the solutions were dried, and then added 0.1 mL concentrated HNO_3, and diluted to 10 mL with deionized water (resistivity of 18 MΩ cm^{-1}). Total 21 elements (Al, Fe, Mn, Mg, Ti, Sc, Na, Sr, Ca, Co, Cr, Ni, Cu, Pb, Zn, Cd, V, S, As, Se, and Sb) were determined by inductively coupled plasma atomic emission spectroscopy (ICP-AES, model, ULTIMA, made by JOBIN-YVON Company, France). The detailed analytical procedures were given elsewhere (Zhuang et al., 2001; Sun et al., 2004).

3. Results and discussion

3.1. Dust episodes observed during spring 2004

Fig. 2 showed the time series plot of the concentration of Al in TSP. Since Al is widely used as an element tracer for the crustal part of aerosols, the dust episodes could be well clarified by the dashed lines in Fig. 2. Thus samples collected during 9–10 March and 27–30 March were grouped into two categories, standing for DS1 and DS2, respectively. The source areas of these two dust events were identified by MODIS (http://rapidfire.sci.gsfc.gov/), which shows that DS1 is likely from the eastern Mongolia, while DS2 from the Gobi Desert in Mongolia (Fig. 1).

Meteorological variables of interest for transport and transformation of air pollutants mainly include wind speed, mixing depth, temperature, and RH. The detailed information of these meteorological variables was shown in Table 2. The average wind speeds were similar during the two dust episodes, while the mixing depth was relative higher in DS2 (Table 2), indicating that more crustal species might be transported with the invasion of DS2. RH and cloud coverage values in DS1 were about 50% and 35% higher than those in DS2 (Table 2). The higher RH, higher cloud coverage, and lower mixing depth in DS1 might allow more pollutants captured and more chemical transformations occurred during the transport of dust particles.

3.2. Spatial patterns in non-dust days

3.2.1. Spatial pattern of the aerosol mass

The economy, climate, topography, and emission sources varied from one site to another (Table 1),

which could lead to the different air quality among these cities. The range and mean concentrations of $PM_{2.5}$ and TSP at the five sites are presented in Table 3. It showed that the aerosol mass peaked in different days at different sites during non-dust period, indicating that the inter-site influence was weak and each site was mainly under the influence of those local emissions. The mean concentrations of $PM_{2.5}$ were higher at the coastal sites (140 $\mu g\,m^{-3}$ at QD and 133 $\mu g\,m^{-3}$ at SH, Table 3), and lower at the county site, DL (60 $\mu g\,m^{-3}$, Table 3). The mean concentrations of TSP followed the order of SH > YL > BJ > QD > DL. This variation suggested that the particulate pollution was the most serious in SH, and was the slightest in DL. SH, located in the east coast of China, is known as the most developed city with the largest gross domestic product (GDP), while DL, located near the sand land, is a small county with the lowest GDP (Table 1). This indicates that GDP, the indicator of city economy, might explain some of the spatial distribution of aerosols. The air quality in a given area might relate more to the local emissions than to the long-range transport in non-dust days.

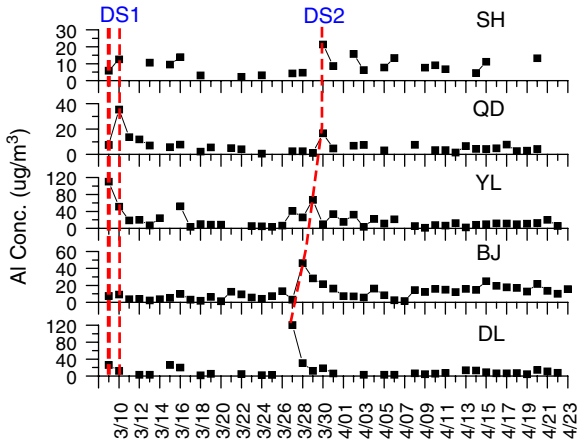

Fig. 2. Daily average concentrations of Al in TSP samples at five sites during the dust season.

3.2.2. Spatial pattern of the aerosol composition

A parameter of CD (coefficient of divergence) could be used to judge the similarity or difference in the concentrations of various chemical components in aerosols from different sites. CD is defined as (Park and Kim, 2004):

$$CD_{jk} = \sqrt{\frac{1}{p}\sum_{i=1}^{p}\left(\frac{x_{ij}-x_{ik}}{x_{ij}+x_{ik}}\right)^2},$$

where x_{ij} represents the average concentration for a chemical component i at site j, j and k represent two sampling sites, and p is the number of chemical components. If the CD approaches zero, the data from the two sites are considered to be similar. If the CD approaches one, they are considered to be much different.

Mean concentrations of the particulate and related ionic and element species in non-dust days were employed in the CD calculation and the results are shown in Fig. 3. CD values were larger between DL and other sites, and smaller among BJ, QD, and SH, indicating that the chemical feature of aerosols in the small undeveloped county might be very different from those in large developed cities irrespective of their geographic location. Fig. 3 showed that the CD values did not show any correlations with the inter-site distance, verifying that all sites in the network might be mainly influenced by numerous local sources and weakly influenced by the long-range transport among sites in non-dust days.

Table 3
Range and mean concentrations of $PM_{2.5}$ and TSP at five sites during dust and non-dust days

	Range of $PM_{2.5}$ and TSP concentrations ($\mu g\,m^{-3}$) (date on which the maximum occurred, mean concentration)				
	DL	YL	BJ	QD	SH
DS1					
$PM_{2.5}$	70–208 (3/9,139)	145–326 (3/10,236)	225–393 (3/9,303)	142–465 (3/10,283)	161–161 (3/10,161)
TSP	201–505 (3/9,353)	919–1996 (3/9,1458)	478–508 (3/9,493)	305–1081 (3/10,680)	479–479 (3/10,479)
$PM_{2.5}$	104–1732 (3/27,403)	152–497 (3/29,252)	156–286 (3/29,213)	137–137 (3/30,137)	106–126 (3/30,116)
TSP	580–3833 (3/27,1632)	425–2639 (3/29,1105)	419–879 (3/29,613)	312–312 (3/30,12)	286–409 (3/30,347)
ND					
$PM_{2.5}$	10–149 (3/15,60)	19–296 (4/21,117)	10–255 (4/15,103)	70–480 (3/25,140)	73–218 (4/2,133)
TSP	26–463 (3/30,153)	21–968 (3/16,269)	40–512 (4/18,240)	80–564 (3/11,209)	133–444 (4/20,278)

In order to show the spatial pattern clearly, the chemical species were grouped into six classes, representing crust, secondary, sea salt, smoke, heavy metals, and carbonaceous aerosol, respectively. Their concentrations were estimated from the measured concentrations of ions and elements. The method of the calculation were shown below: (1) crust = Al/0.08; (2) secondary = $NH_4^+ + NO_3^- + SO_4^{2-}$; (3) sea salt = 2.54*(Na−0.3Al), here (Na−0.3Al) stands for the non-crustal Na and this part of Na is assumed to be solely from the sea-salt (Chan et al., 1997); (4) smoke (actually, non-crustal *K*) = *K*−0.25Al (Chan et al., 1997); (5) metals = the sum of the mass of all non-crustal/non-sea-salt elements measured by ICP-AES (*S* and *K* were excluded from this sum); and (6) carbonaceous aerosol, roughly estimated with a mass balance, neglecting those minor components and H_2O. The relative contributions of the above six main constituents in $PM_{2.5}$ and TSP in DS1, DS2 and ND were shown in Fig. 4.

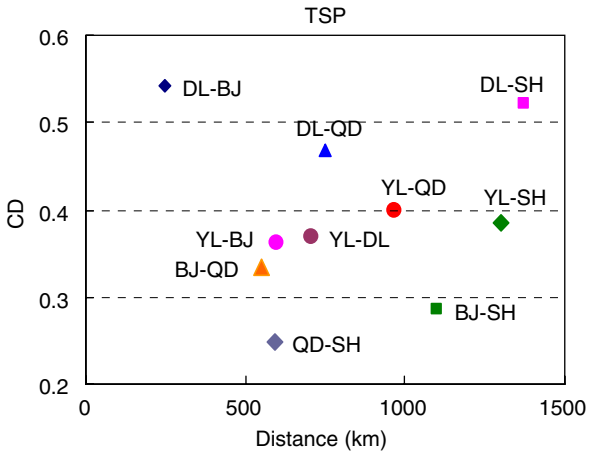

Fig. 3. The CD values for TSP at the paired sites (site 1–2) in non-dust days.

It showed that the spatial patterns for the composition in $PM_{2.5}$ and TSP were very similar during non-dust period. At each site, crust, secondary, and carbonaceous aerosols were the main contributors to the PM mass. The mass fraction of the crust decreased from the inland sites near the dust source (DL and YL) to the coastal sites far away from the dust source (QD and SH). The crustal component comprised 65% of $PM_{2.5}$ at DL, which was nearly four time higher than those at QD (14%) and SH (16%). This result indicated that particle emission from the arid area was the main source for crustal component in aerosols even during the non-dust period. The fraction of the secondary components generally displayed a spatial variation contrary to that of the crust. At urban sites in the large cities, either continental (BJ) or coastal (QD and SH), secondary aerosol averaged to 18–32% of the $PM_{2.5}$ mass, while at sites in the county (DL) and in the middle city (YL), it only contributed 8–10% to the $PM_{2.5}$ mass. Secondary

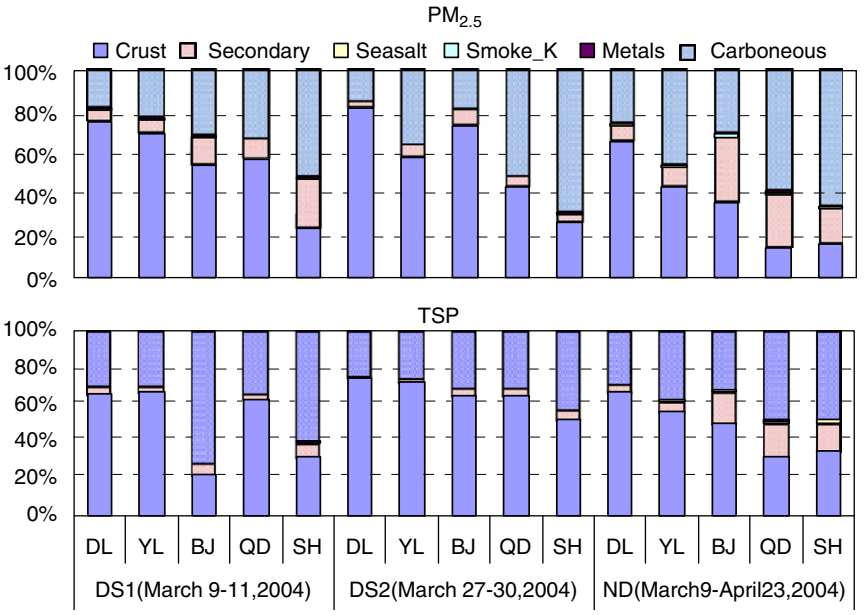

Fig. 4. Composition of $PM_{2.5}$ and TSP at five sites during DS1, DS2, and ND periods.

components are known to be mainly from anthropogenic sources, likely the oxidation of SO_2/NO_X emitted from coal burning/traffic emission. The GDP in BJ, QD, and SH is 10–1000 times higher than that in DL and YL, and the population is 2–130 times higher (Table 1), therefore, more fuels (coal/oil/gasoline) are expected to be used in BJ, QD, and SH both for economy development and for the residential life, resulting in the abundant of the secondary aerosol in the large developed cities. The spatial variation of the carbonaceous aerosol was similar to that of the secondary aerosol, indicating that they were mainly from the anthropogenic emissions, such as coal burning, traffic, cooking, and industry emissions (Dan et al., 2004; Hou et al., 2006). It should be mentioned that the contribution of the carbonaceous aerosol was unusually higher in YL, especially in $PM_{2.5}$ samples. This fact might be explained by the three large coal mines located around YL (www.sxyl.gov.cn). As described above, the different chemical composition was related to the city characteristics and could give useful clues on the major sources around the cities.

3.2.3. Spatial pattern of the aerosol acidity

The relationship between the equivalent concentrations ($\mu eq\,m^{-3}$) of the total cations ($\sum+$) and the total anions ($\sum-$) could be used to denote the aerosol acidity. The linear regression characteristics of $\sum+$ and $\sum-$ at the five sites in non-dust days was compared in Table 4. As indicated by the slope of the regression line, acidity was lower in areas near the dust source (DL and YL), and higher in densely populated and industrialized areas (BJ, QD, and SH). This was consistent with the abundance of the basic crustal components in DL and YL, and the abundance of the acidic secondary sulfate and nitrate in BJ, QD, and SH (see Section 3.2.2). The poor correlations between $\sum+$ and $\sum-$ for TSP samples in DL and YL might suggest the existence of carbonate aerosols, which could not be quantified by IC in this study. Carbonate, possibly in the form of $CaCO_3$ and/or $MgCO_3$, is abundant in the semiarid and arid area in north China. It can react with acidic species and mitigate the acidifying progress (Wang et al., 2002; Wang et al., 2005a, b). On the contrary, the large amount of the acidic secondary components, mainly from anthropogenic emissions, in aerosols in large developed cities would quicken the acidifying progress and make the environment more susceptible. Regulations should be taken for the sake of the sustainable development of the cities.

3.2.4. Spatial pattern of the aerosol size distribution

Fig. 5 showed that the secondary aerosol was mainly confined to the fine particles in non-dust days, with $PM_{2.5}$/TSP in the range of 0.55–0.97. Except SH, the $PM_{2.5}$/TSP ratio of the secondary aerosol increased along the northwest-southeast line, i.e. DL < YL < BJ < QD. It is well known that the secondary aerosol in the fine mode is mainly from the oxidation of pollution gases, SO_2 and NO_X, while in the coarse mode it is largely related to primary emissions from soil, road dust, and sea-salt etc. The high values in BJ and QD might be related to the high levels of SO_2 and NO_X from industry, traffic, and residential heating in these developed cities. Besides, the atmospheric humidity might control the distribution to some extent. High RH can favor the formation of sulfate and nitrate from SO_2 and NO_X on the one hand, and restrict the suspension of coarse particles on the other hand. The mean RH was over two times higher at coastal sites (QD 66%) than at inland sites (YL 21%). This might contribute to the high percentage of

Table 4
The relationship between equivalent concentrations of total cations (Σ+) and total

	$PM_{2.5}$			TSP		
	Linear regression equation	r^a	NO[b]	Linear regression equation	r^a	NO[b]
DL	$\Sigma+ = 0.02 + 0.93\ \Sigma-$	0.94	46	$\Sigma+ = 0.10 + 1.03\ \Sigma-$	0.56	36
YL	$\Sigma+ = 0.03 + 1.14\ \Sigma-$	0.82	45	$\Sigma+ = 0.24 + 0.92\ \Sigma-$	0.70	46
BJ	$\Sigma+ = 0.10 + 0.68\ \Sigma-$	0.94	50	$\Sigma+ = 0.13 + 0.68\ \Sigma-$	0.98	50
QD	$\Sigma+ = 0.02 + 0.66\ \Sigma-$	0.96	45	$\Sigma+ = 0.06 + 0.66\ \Sigma-$	0.95	37
SH	$\Sigma+ = -0.03 + 0.75\ \Sigma-$	0.99	32	$\Sigma+ = 0.04 + 0.67\ \Sigma-$	0.97	22

[a]Correlation coefficient.
[b]Number of samples.

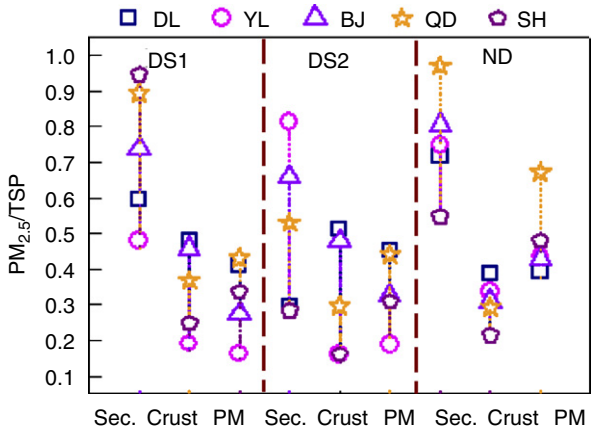

Fig. 5. The $PM_{2.5}$ to TSP concentration ratio of secondary, crust, and PM at five sites in DS1, DS2, and ND (Sec.: secondary; PM: particulate mass).

secondary components in the fine mode in QD. Among the five sites, SH had the lowest $PM_{2.5}$/TSP ratio of the secondary aerosol. This exception might due to the evaporation of nitrate/ammonium from the fine particles caused by the high temperature in SH. Besides, it probably related to the sampling site at Shanghai, which was unfortunately near a place that was unexpected in big construction during the sampling period.

Crust was mainly distributed in the coarse mode, with $PM_{2.5}$/TSP in the range of 0.21–0.39. This ratio showed a spatial variation of DL > YL > BJ > QD > SH, which was just opposite to that of the secondary aerosol. However, the size distribution of crust exhibited weak spatial variation compared to the secondary aerosol, suggesting that the natural crustal sources were similar within China, and the different characteristics of aerosols was more related to the local anthropogenic emissions.

The average ratio of $PM_{2.5}$ to TSP for the particle mass (PM) was in 0.39–0.67, which was roughly between those of secondary and those of crustal components. The ratio showed that the continental sites (DL, YL, BJ) had higher fraction of the coarse particles than the coastal sites (QD, SH). This might relate to the humid atmosphere in coastal areas, which could enhance the wet deposition of larger particles. The distribution of PM was similar between the undeveloped county site (DL) and developed metropolitan site (BJ), indicating that the urban activities could contribute to the fine particles from the vehicular and industrial emissions as well as to the coarse particles from the road dust raised by the vehicular motion and the construction activities.

3.3. Impacts of the dust emissions from the upstream and from the transport pathways

3.3.1. Impact on the aerosol concentrations

Table 3 showed that during DS1 period, the mean $PM_{2.5}$ concentrations at DL, YL, BJ, QD, and SH were 2.32, 2.02, 2.94, 2.02, and 1.21 times of those in the non-dust days; For TSP it was 2.31, 5.42, 2.05, 3.25, and 1.72, respectively. During DS2 period, the corresponding values were 6.72, 2.15, 2.07, 0.98, 0.87 for $PM_{2.5}$ and 10.67, 4.11, 2.55, 1.49, 1.25 for TSP, respectively. The increase was weaker and with less variation among the five sites in DS1 than in DS2, indicating that DS1 was more widely spread, while DS2 was stronger. Maximum increase was observed at sites adjacent to the source areas of dust storm (DL and YL). The elevation of the particulate mass was more obvious in TSP than in $PM_{2.5}$, although the fine particles are more favorable for the long-range transport. This suggested that most of the observed increase is likely to be ascribed to the crustal components, which are known to be distributed more in the coarse particles.

3.3.2. Impact on the aerosol composition

Fig. 6 showed the change of the mass percentages of the crust and the secondary components in aerosols in DS1 and DS2 to that in non-dust days. Generally, the fraction of the crustal components increased during the dust episodes, while the secondary components decreased. This might be due to the dilution of the anthropogenic pollution species by the mineral particles during the dust episodes (Guo et al., 2004a, b). The increase of the crustal components was more obvious in $PM_{2.5}$. This might be related to the fact that the secondary components, mostly from the anthropogenic pollution sources, were mainly presented in the fine mode in non-dust days, and crustal components in the fine particles could be preferably subjected to long-range transport. Different from the crustal components, the decrease of the secondary aerosol was more obvious in TSP, indicating that the secondary components might be formed, especially on the fine particles, during the long-range transport of dust particles.

Interestingly, the increase of the crustal fraction and the decrease of the secondary fraction was weak at sites near the dust sources (DL and YL), while it

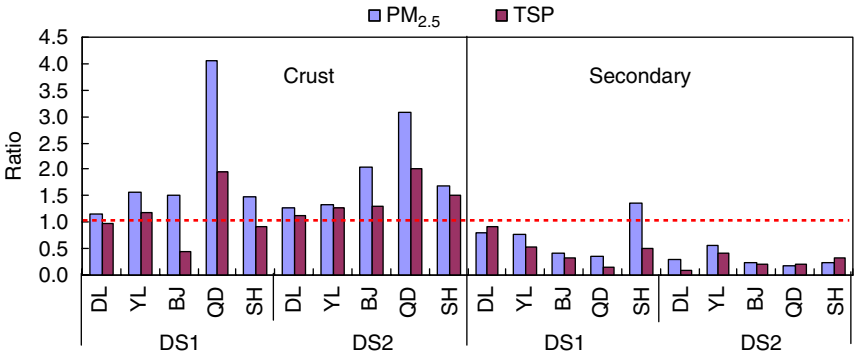

Fig. 6. The dust to non-dust ratio of the mass percentages of crust and secondary components in $PM_{2.5}$ and TSP at five sites in DS1 and DS2.

was obvious in downwind areas, especially in QD. This suggested that the chemical characteristics of the aerosols near the dust sources were similar in the dust days and in the non-dust days, i.e. aerosols might be controlled by dust emissions whether or not there was dust storm. On the contrary, the characteristics of the aerosols in the downwind area showed large differences between the dust and the non-dust days, indicating that aerosols might be largely controlled by the local anthropogenic emissions in the non-dust days, and by the transported dust in the dust days. The higher elevation of the crustal components in QD than in SH might be mainly due to the closer distance from the dust sources to QD than that to SH.

Fig. 6 also showed that the decrease of the secondary aerosol was relative minor in DS1 than in DS2, indicating that the formation of the secondary components, sulfate and/or nitrate, was favored in DS1 due to the higher RH, higher cloud coverage, and the low mixing depth in this period (Table 2). Notably, the fraction of the secondary aerosols even increased in $PM_{2.5}$ in SH. This might be related to the long distance from the dust sources to SH, which could provide sufficient time for the chemical transformation process and more secondary aerosols.

3.3.3. Impact on the aerosol acidity

Fig. 1 suggested that DS2 was a good example of the correlation among sites. During this period, large increases in Al concentrations were detected at all sites with a slight lag in time of onset due to the west to east progression of the episode-forming meteorological conditions. Fig. 7 showed that the acidity of the particles, suggested by the equivalent ratio of the total cations ($\sum+$) to the total anions

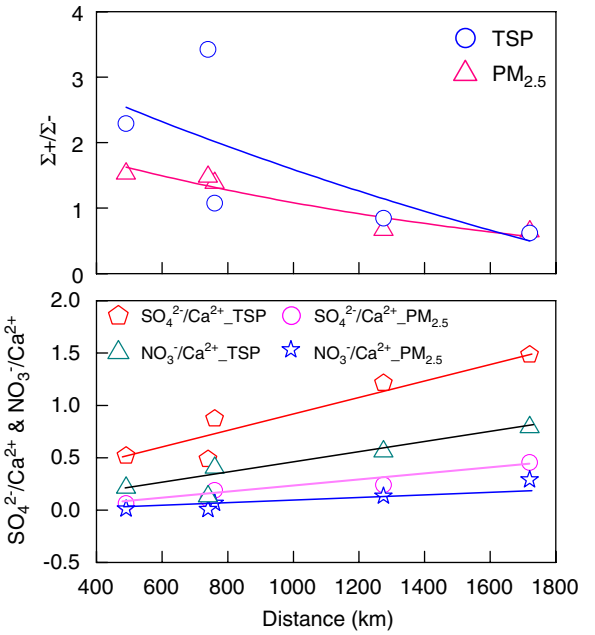

Fig. 7. The change of $\Sigma+/\Sigma-$ ($\mu eq\,m^{-3}$) and SO_4^{2-}/Ca^{2+} and NO_3^-/Ca^{2+} ($\mu g\,m^{-3}$) with the distance from the dust sources to the downwind areas in DS2.

($\sum-$) of the water-extract of the particles (Wang et al., 2005a, b), changed as the episodic condition progressed eastward. Particles were getting more and more acidic along the transport of the dust particles. In the east coastal area (SH), the $\Sigma+/\Sigma-$ ratio was as low as 0.5, which was about 88% and 80% lower than those in dust source area for TSP and $PM_{2.5}$, respectively. This result might be due to the mixing and interaction of the basic crustal particles with acidic aerosols or gases emitted from heavy industry and densely populated areas in the transport pathway of the dust parcels. Fig. 7

showed that the concentration ratio of SO_4^{2-}/Ca^{2+} and NO_3^-/Ca^{2+} increased from the areas near the dust source (DL, YL) to downwind coastal areas (QD, SH), verifying that the reactions of $SO_2/NO_X/$ sulfate/nitrate with the dust particles containing Ca (mainly as $CaCO_3$) occurred during the transport (Wang et al., 2005b). The $\Sigma+/\Sigma-$ ratio exhibited sharper decrease in TSP than in $PM_{2.5}$. Accordingly, the ratios of SO_4^{2-}/Ca^{2+} and NO_3^-/Ca^{2+} increased markedly in TSP, indicating that the reactions mentioned above was favored on the coarse particles. One reason might be that coarse particles are more likely to react with acidic species for its basic character. The other one might relate to the reaction mechanism. Fine particles are known to have larger surface for the same mass. However, the reaction was not favored on the fine particles, indicating that the reaction into the bulk of the particles was possible. RH plays an important role in determining whether the reaction can penetrate inside particles due to the solubility and hygroscopy of the $Ca(NO_3)_2$ and $CaSO_4$ formed. It was found that the reaction of $CaCO_3$ with HNO_3 continued in the presence of water vapor at 20% RH without any evidence for surface saturation (Goodman et al., 2000). The average RH was 22% in DS2, demonstrating that the reaction could take place inside dust particles in this study. In this case, sulfate/nitrate formation increases linearly with the mass of the sample (Usher et al., 2003). Therefore, the favored reaction in TSP could be well interpreted.

Fig. 7 showed that the slope of the regression line of SO_4^{2-}/Ca^{2+} was higher than that of NO_3^-/Ca^{2+}, indicating that the sulfate formation was prominent compared to the nitrate formation. The lower atmospheric concentration of NO_2 in China could partly explain the result. However, the different formation mechanism of sulfate and nitrate might be the key factor. Previous studies showed that NO_2 had lower capacities than SO_2 in the reaction with mineral particles (Mamane and Gottlieb, 1989, 1992). The exact mechanism should be further investigated in the future.

3.3.4. Impact on the aerosol size distribution

Fig. 5 showed that 40–67% of PM was in the fine fraction in the non-dust days, while it was 16–45% in the dust days. The decrease of the fine fraction in the dust days suggested that the transported dust was mainly in the size range of $>2.5\,\mu m$. Secondary components shift to the coarse mode, while crustal components shift to the fine mode during the dust episodes. These shifts might be mainly related to the dilution of the secondary components by the invaded crustal components. The dilution was more obvious in the fine mode, because the secondary aerosols were mostly distributed in the fine mode and the crustal components in the fine mode were easily subjected to the long-range transport. Notably, there were some exceptions. More than 90% of the secondary components were confined to $PM_{2.5}$ in QD and SH in DS1. This might be possibly attributed to the formation of sulfate/nitrate on the surface of fine particles during the transport, from inland sandy area to the coastal cities. The high temperature, high cloud coverage and the low mixing depth in DS1 favored this transformation (Table 2). However, the crustal components shift to the coarse mode in YL during the dust episodes. Since much of the wind-blown dust from the local sources was in the larger particle size, and the long-range transport dust was largely in the fine mode, the shift of crustal components in YL might indicate that a large part of mineral aerosols was from the local emissions during the dust episodes for the high wind speed and the dry sandy ground. The relative contribution of the local and the long-range transport to the PM needs to be further studied.

3.4. Source apportionment

3.4.1. Crust vs. pollution suggested by enrichment factor

To provide a first indication on the extent of the contribution of the anthropogenic emissions to the element/ion levels in the atmosphere, the enrichment factor (EF) has been calculated for a series of elements and ions, using Al as reference element and the crustal abundance given by Taylor (1964). The formula used is

$$EF_X = (X/Al)_{aerosol}/(X/Al)_{crust},$$

where $(X/Al)_{aerosol}$ and $(X/Al)_{crust}$ represent the relative concentration of a certain species (X) to Al in the aerosol and crust, respectively. Species with EFs close to unity have a strong natural component, while species with high EFs have mainly an anthropogenic origin.

Mean EFs for those species in $PM_{2.5}$ samples at BJ were presented in Fig. 8. The EF values for Na, Ti, V, Mg, Fe, Mn, Co, Sr, Ca, and Cr, were mostly less than 5, indicating that these ten elements were largely contributed by the mineral dust. Compared with the dust-derived elements, the EF values of As,

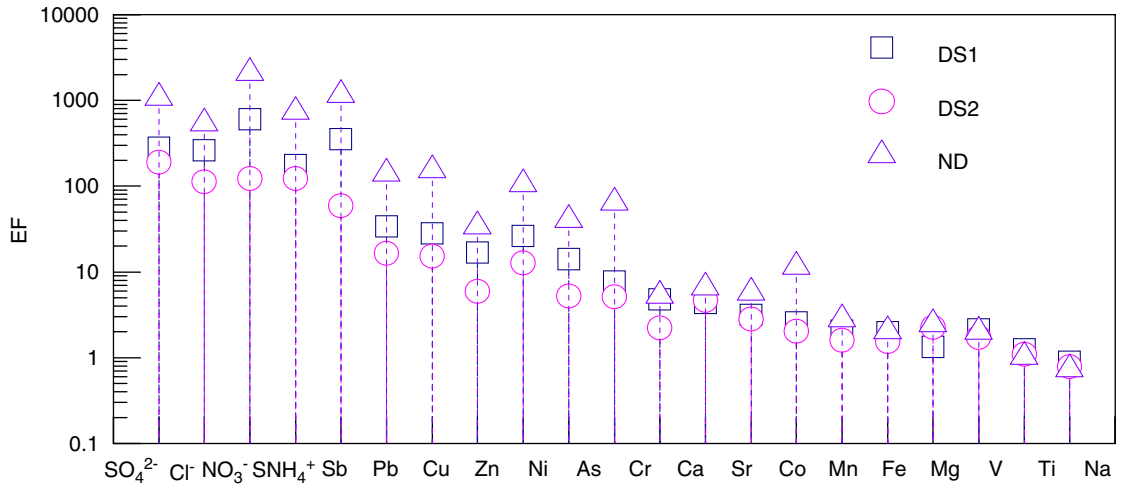

Fig. 8. Enrichment factors (EF) for species in $PM_{2.5}$ at Beijing during spring 2004.

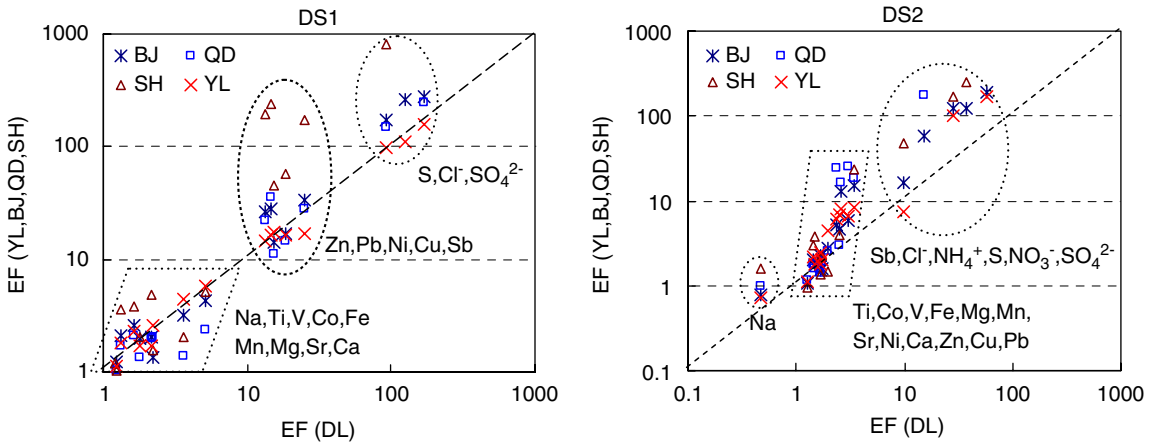

Fig. 9. The relationship between enrichment factors at DL and the other sites for $PM_{2.5}$ during DS1 and DS2 periods.

Ni, Zn, Cu, Pb, and Sb were larger than 5, suggesting the significant influences of the non-crustal sources on these elements. The EF values for SO_4^{2-}, S, Cl^-, NO_3^-, and NH_4^+ were generally larger than 100, indicating that these species were often enriched through anthropogenic emissions. Fig. 8 also showed that the EFs for a certain species often followed the order of ND > DS1 > DS2, and the variation among different periods was more significant for the species with larger EF values. This result suggested that a certain amount of the pollution components was wiped off by the invaded dust parcels, and this process appeared to be more significant in DS2, which was stronger than DS1.

In order to show the interaction between the pollution and the crustal components during the long-range transport of the dust aerosols, the EFs for a certain species in $PM_{2.5}$ at different sites were compared in Fig. 9, and their relationship was shown in Table 5. Fig. 9 showed that the EFs of pollution species (SO_4^{2-}, S, Cl^-, NO_3^-, NH_4^+) had larger spatial variations than those of the crustal species (Na, Ti, V, Mg, Fe, Mn, Co, Sr, Ca), suggesting that the impact of the pollutants emitted from the local sources or the sources in the transport pathway was spatially different and could not be neglected. The EFs of the pollution species were higher in DS1 than in DS2 (Fig. 9), indicating that more pollutants might be captured or formed during the long-range transport of dust aerosols in DS1. It also indicated that more local pollutants were wiped off by the intrusion of the dust particles in DS2 for its stronger strength. The EFs of the crustal species (EF = 1–10) showed larger spatial

variations in DS1 than in DS2 (Fig. 9), indicating that the local contribution to the crustal components might prevail in DS1, while the long-range transport controlled more in DS2.

Significant correlations were observed for the EFs among different sites during the dust episodes (Table 5), indicating the impact of the dust emission from the upstream and from the pathways on the local environment. The slopes of the regression lines were mostly higher than 1 (Table 5), suggesting the accumulation of the pollutants on the transport pathway. The different slopes among YL, BJ, QD, and SH might be associated with the different transport distances and the amount of the pollutants emitted from the anthropogenic activities on the transport pathway. The species excluded in deriving the regression lines were also listed in Table 5. It showed that they might be mainly in the form of ammonium nitrate and ammonium chloride. Their deviations suggested that they could not be transported for a long distance and mainly controlled by the local sources.

Table 5
Linear regression equation and correlation coefficient (r) between enrichment factors at DL and the other site for $PM_{2.5}$ during DS1 and DS2 periods

	Linear regression equation	r	Excluded species[a]
DS1	EF (YL) = 0.95 EF(DL)	0.9970	$NO_3^-NH_4^+$
	EF (BJ) = 1.82 EF(DL)	0.9899	$NO_3^-NH_4^+$
	EF (QD) = 1.50 EF(DL)	0.9946	$NO_3^-NH_4^+Cl^-$
	EF (SH) = 8.92 EF(DL)	0.9910	$NO_3^-NH_4^+Cl^-$
DS2	EF (YL) = 3.02 EF(DL)	0.9870	$NO_3^-NH_4^+Cl^-$
	EF (BJ) = 3.42 EF(DL)	0.9882	Cl^-
	EF (BJ) = 3.42 EF(DL)	0.9466	$NO_3^-Cl^-$
	EF (SH) = 6.28 EF(DL)	0.9917	$NH_4^+Cl^-$

[a]Species excluded in deriving the relationship for their deviation to the linear line.

3.4.2. Local vs. long-range transport suggested by positive matrix factorization

The PMF receptor model was applied to the total dataset of 409 aerosol samples using 21 input variables, including PM, Na^+, NH_4^+, K^+, Mg^{2+}, Ca^{2+}, Cl^-, NO_3^-, SO_4^{2-}, Sr, Pb, Ni, Fe, Mn, Mg, V, Ca, Cu, Ti, Al, and Na. Other variables were excluded either for the high missing percentage or the low signal-to-noise ratio. A unique four-factor model was resolved. The difference between the Q-value obtained (11,495) and the theoretical Q-value (8463) was within 50% of the theoretical

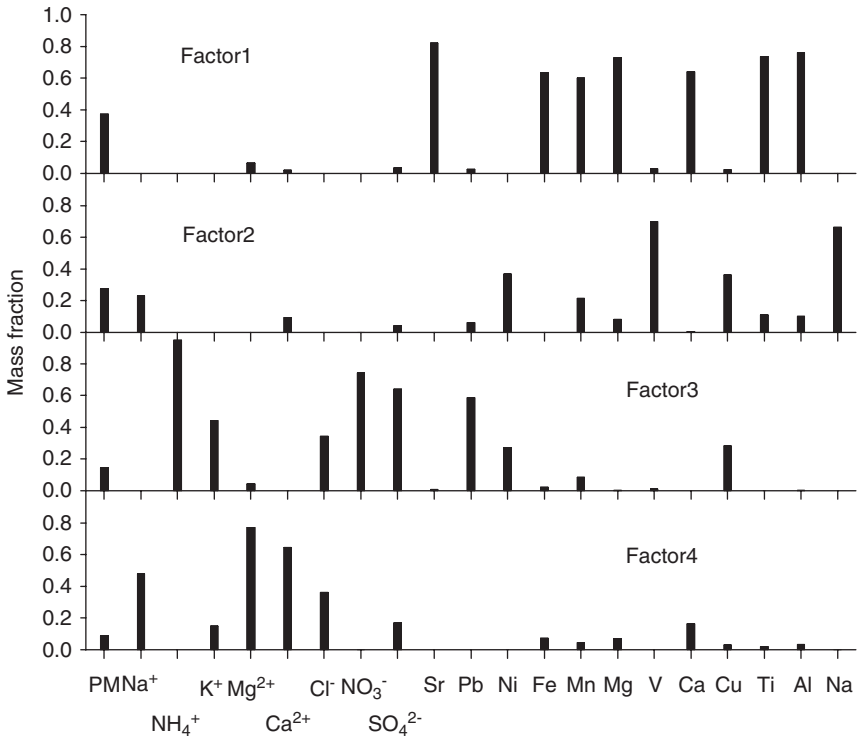

Fig. 10. The distribution of species concentrations among the four factors.

Q-value. Chemical profiles (in $\mu g\,m^{-3}$) were derived directly from the F-Factor matrix (factor loading matrix). The concentration ratio of the employed variables in each factor to their measured concentrations were calculated based on the F-Factor matrix and presented in Fig. 10.

The G-Factor matrix (daily factor score matrix) was regressed against the measured concentrations of PM and chemical species using multiple linear regression. The regression coefficients were multiplied by the daily factor scores to determine the daily concentrations (in $\mu g\,m^{-3}$) of the species in the four factors. The sum of the calculated concentrations in the four factors represents the predicted concentrations of those species. Representative comparison of the measured concentrations of PM, Al, SO_4^{2-}, NO_3^- with predicted ones was shown in Fig. 11. The slopes of the regression lines are near to 1, and the correlation coefficients were in the range of 0.93–0.98. This agreement between the measured and calculated concentrations indicated the good fits among the chemical species and factors.

Factor 1 has high loadings for Sr, Fe, Mn, Mg, Ca, Ti, and Al (Fig. 10). As suggested in Figs. 8 and 9, most of these elements have EFs lower than 5, indicating that Factor 1 is primarily of crustal origin. The contribution of this factor to the PM was more than three times higher during dust episodes (183.9, 322.2, and 53.1 $\mu g\,m^{-3}$ in DS1, DS2, and ND, respectively) when long-range transport was generally more efficient. Besides, it was correlated with wind speed ($r = 0.363$, sig. (two-tailed) $= 0.000$). Thus Factor 1 could represent remote or regionally transported dust. Factor 2 had high loadings on V, Na, Mn, Ni, Cu, and weak loadings on Mg, Ti, Al, Pb (Fig. 10). V, Na, Mn, Mg, Ti, and Al were largely of crustal origin; Pb and Ni could be from the oil/gasoline burning; Cu could be from the brake lining. Therefore, Factor 2 was presumed to represent the local dust associated with those from traffic activities. Factor 3 was highly loaded with NH_4^+, NO_3^-, SO_4^{2-}, Pb, K^+, and weakly loaded with Cl^-, Ni, Cu (Fig. 10). This factor could be identified as the secondary anthropogenic sources, likely coal burning (SO_4^{2-}, Pb, Ni), traffic emission (NH_4^+, NO_3^-, SO_4^{2-}, Pb), biomass burning (K^+, Cl^-), and refuse incineration (Cu, Cl^-, Pb) (Bandhu et al., 2000). The contribution of this factor to the PM was weakened during the dust episodes (25.2, 7.78, and 35.3 $\mu g\,m^{-3}$ in DS1, DS2, and ND, respectively). Moreover, it was anti-correlated with wind speed ($r = -0.154$, sig. (two-tailed) $= 0.002$), suggesting that the particles associated with this factor might be mainly from local sources. Therefore, Factor 3 is identified as the local secondary sources from anthropogenic emissions. Factor 4 is highly loaded with Mg^{2+}, Ca^{2+}, Na^+,

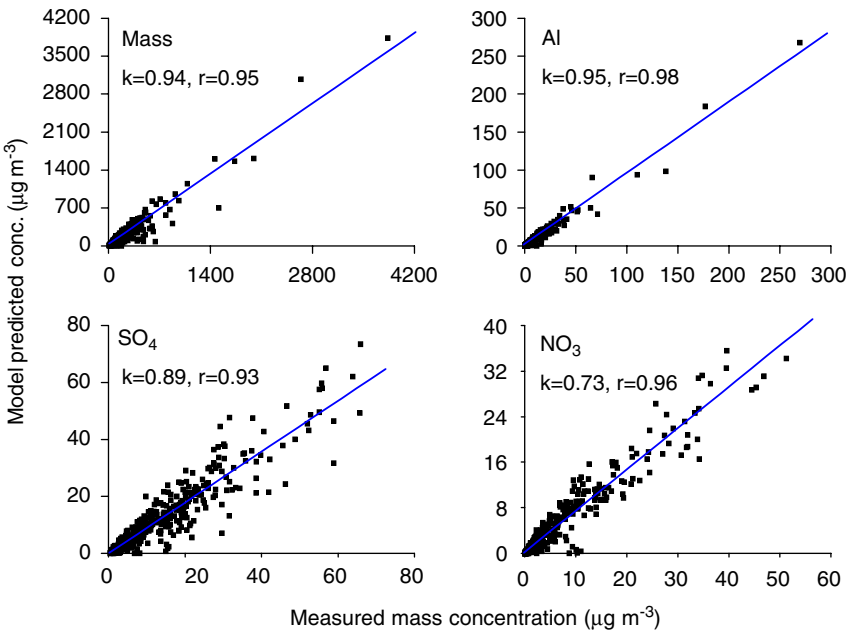

Fig. 11. The relationship between the measured and predicted concentrations of PM, Al, SO_4^2, NO_3^- in all the aerosol samples.

Cl^-, and weakly loaded with SO_4^{2-}, K^+(Fig. 10). This factor was assumed to be linked to the soluble dust from salt lakes in the arid and semiarid areas in northwestern China. But based on the profile of Factor 4, the calculated mass ratios of Mg^{2+}, Ca^{2+}, Cl^-, and SO_4^{2-} to ($K^+ + Na^+$) were 0.397, 5.866, 4.488, and 5.184, respectively, which were substantially higher than the corresponding ratios of 0.083, 0.280, 1.354, and 1.193 in the salt-dust samples in China (Abuduwaili and Guijin, 2006), indicating that there must be the adsorption of acidic pollutants or/and the formation of secondary chloride and sulfate aerosols on the alkaline salt-dust particles (pH = 8.7, Abuduwaili and Guijin, 2006) during the long-range transport. Thus, this factor could stand for the anthropogenic pollution source from long-range transport. Fig. 10 showed that Factor 1, Factor 2, Factor 3, and Factor 4 contributed about 37.4%, 27.5%, 14.3%, and 8.9% to PM, respectively, indicating the predominance of crustal components in aerosols in the dust season in China.

As indicated by the sources attributed to each factor, the concentration ratio of PM in (Factor 1 + Factor 4)/(Factor 1 + Factor 2 + Factor 3 + Factor 4) could indicate the contribution of the sources from the upstream and from the transport pathways to the PM. Similarly, the concentration ratio of crust (Al/0.08) in Factor 1/(Factor 1 + Factor 2) and the ratio of the secondary aerosol (ammonium + nitrate + sulfate) in Factor 4/(Factor 3 + Factor 4) could indicate the contribution of the sources from the upstream and from the transport pathways to the crust and the secondary aerosols, respectively. In this way, the contribution of the sources from the upstream and from the transport pathways to PM, the crust, and the secondary aerosols were calculated for all the samples, and the results were presented in Fig. 12. It was found that the sources from the upstream and the pathways transported could account for about 49%, 82%, and 28% of PM mass, crust, and secondary aerosol, respectively during the entire period, indicating that secondary aerosols might be mitigated by the local management for their large contribution from the local sources (72%), while the crustal components could not be easily controlled due to their large contribution from outside area (82%). Fig. 12 also showed that the contribution of the source from the upstream to PM, crust, and secondary aerosols decreased from the regions near the dust source (DL, YL) to the regions far away (BJ, QD, SH),

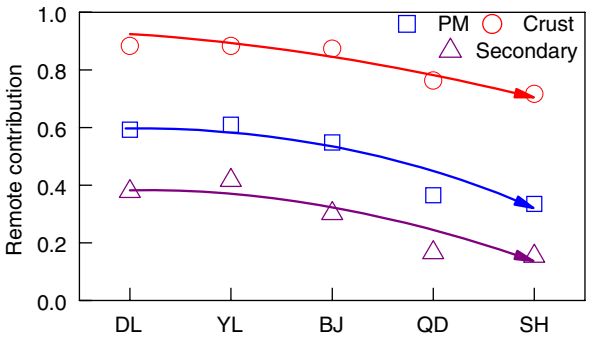

Fig. 12. Remote contribution to PM, crust, and secondary aerosols for all the samples collected.

suggesting the impact of dust storms from the upstream and from the transport pathways on the local environment. This finding could provide useful information on the strategies taken for controlling PM and the related crustal and secondary components in the region.

4. Conclusions

Asian dust aerosols were collected at five locations in China along the pathways of the dust event in spring 2004. During this period, two dust events (DS1: 9–10 March and DS2: 27–30 March) were identified based on the concentrations of Al in $PM_{2.5}$ and TSP. DS1 was widely spread, while DS2 was stronger. Mass concentrations, chemical compositions, size distributions, and sources of the aerosols were examined.

Particulate pollution was found to be associated with the city economy (GDP). The crust, the secondary, and the carbonaceous components were the main fractions in the particles. The mass fraction of the crust decreased from the dust source to the downwind coastal sites, while those of the secondary and the carbonaceous components increased. During the two dust events, significant increase in particle concentration were observed at all the sites, and a large part of the secondary components was diluted by the crustal components, especially in the fine particles. The secondary aerosol shift to the coarse mode and the crustal components shift to the fine mode during the dust episodes. Particles were getting more and more acidic as the episodic dust progressed eastward, indicating the mixing and reaction of basic crustal particles with the acidic gases and/or the pollution particles during the transport.

Dust particles were found to react with SO_2/NO_X/sulfate/nitrate based on the variations of SO_4^{2-}/Ca^{2+} and NO_3^-/Ca^{2+} along the transport pathway. This reaction was favored on the coarse particles in DS1. Moreover, the formation of sulfate was prominent compared to nitrate, suggesting the different formation mechanism of sulfate and nitrate.

EF analysis showed that Mg, Fe, Mn, Co, Sr, Ca, and Cr were largely contributed by the natural crustal sources, while SO_4^{2-}, S, Cl^-, NO_3^-, and NH_4^+ were often enriched through anthropogenic emissions. There were highly significant correlations between the EFs of species at different sites, which suggested that these species derived from the similar sources and shared the similar transport mechanism.

Four factors were resolved by PMF and represented: (1) the transported dust from the upstream or from the pathways, (2) the local dust associated with the traffic activities, (3) the local secondary sources from the anthropogenic emissions, and (4) the transported anthropogenic emissions from the pathways. It was found that the sources from the upstream and the pathways transported could account for 49%, 82%, and 28% of PM mass, crust, and secondary aerosol, respectively, and the contribution decreased from regions near the dust source to regions far away.

Acknowledgments

This work was supported by the National Key Project of Basic Research (Grant no. 2006CB403704), National Natural Science Foundation of China (Grant Nos. 30230310, 20477004, and 40575062), Beijing Natural Science Foundation (Grant No. 8041003), and also in part supported by SKLLQG, the Institute of Earth Environment, and the Swedish International Development Cooperation Agency (SIDA) through the Asian Regional Research Program on Environmental Technology (ARRPET) at the Asian Institute of Technology.

References

Abuduwaili, J., Guijin, M., 2006. Eolian factor in the process of modern salt accumulation in western Dzungaria, China. Eurasian Soil Science 39, 367–376.

Arimoto, R., Ray, B.J., Lewis, N.F., Tomza, U., 1997. Mass–particle size distribution of atmospheric dust and the dry deposition of dust to the remote ocean. Journal of Geophysical Research 102 (D13), 15867–15874.

Bandhu, H.K., Puri, S., Garg, M.L., Singh, B., Shahi, J.S., Mehta, D., Swietlicki, E., Dhawan, D.K., Mangal, P.C., Singh, N., 2000. Elemental composition and sources of air pollution in the city of Chandigarh, India, using EDXRF and PIXE techniques. Nuclear Instruments and Methods in Physics Research B 160, 126–138.

Cao, J.J., Lee, S.C., Zheng, X.D., Ho, K.F., Zhang, X.Y., Guo, H., Chow, J.C., Wang, H.B., 2003. Characterization of dust storms to Hong Kong in April 1998. Water, Air, and Soil Pollution: Focus 3, 213–229.

Chan, Y.C., Simpson, R.W., McTainsh, G.H., Vowles, P.D., Cohen, D.D., Bailey, G.M., 1997. Characterisation of chemical species in $PM_{2.5}$ and PM_{10} aerosols in Brisbane, Australia. Atmospheric Environment 31, 3773–3785.

Chen, S.J., Hsieh, L.T., Kao, M.J., Lin, W.Y., Huang, K.L., Lin, C.C., 2004. Characteristics of particles sampled in southern Taiwan during the Asian dust storm periods in 2000 and 2001. Atmospheric Environment 38, 5925–5934.

Dan, M., Zhuang, G., Li, X., Tao, H., Zhuang, Y., 2004. The characteristics of carbonaceous species and their sources in $PM_{2.5}$ in Beijing. Atmospheric Environment 38, 3443–3452.

Dentener, F.J., Carmichael, G.R., Zhang, Y., Lelieveld, J., Crutzen, P.J., 1996. Role of mineral aerosol as a reactive surface in the global troposphere. Journal of Geophysical Research 101, 22869–22889.

Duce, R.A., Liss, P.S., Merrill, J.T., Atlas, E.L., Buat-Menard, P., Hicks, B.B., Miller, J.M., Prospero, J.M., Arimoto, R., Church, T.M., Ellis, W., Galloway, J.N., Hansen, L., Jickells, T.D., Knap, A.H., Reinhardt, K.H., Schneider, B., Soudine, A., Tokos, J.J., Tsunogai, S., Wollast, R., Zhou, M., 1991. The atmospheric input of trace species to the world ocean. Global Biogeochemical Cycles 5, 193–259.

Fan, X.B., Okada, K., Niimura, N., Kai, K., Arao, K., Shi, G.Y., Oin, Y., Mitsuta, Y., 1996. Mineral particles collected in China and Japan during the same Asian dust-storm event. Atmospheric Environment 30, 347–351.

Fang, M., Zheng, M., Wang, F., Chim, K.S., Kot, S.C., 1999. The long-range transport of aerosols from northern China to Hong Kong—a multi-technique study. Atmospheric Environment 33, 1803–1817.

Goodman, A.L., Underwood, G.M., Grassian, V.H., 2000. A laboratory study of the heterogeneous reaction of nitric acid on calcium carbonate particles. Journal of Geophysical Research 105 (D23), 29053–29064.

Guo, J., Rahn, K., Zhuang, G., 2004a. A mechanism for the increase of pollution elements in dust storms in Beijing. Atmospheric Environment 38, 855–862.

Guo, Z., Feng, J., Fang, M., Chen, H., Lau, K., 2004b. The elemental and organic characteristics of $PM_{2.5}$ in Asian dust episodes in Qingdao, China, 2002. Atmospheric Environment 38, 909–919.

Hou, X., Sun, Y., Zhuang, G., An, Zh., 2006. Characteristics and sources of polycyclic aromatic hydrocarbons and fatty acids in $PM_{2.5}$ aerosols in dust season in China. Atmospheric Environment 40, 3251–3262.

Iwasaka, Y., Yamato, M., Imasu, R., Ono, A., 1988. Transport of Asian dust (KOSA) particles: importance of weak KOSA events on the geochemical cycle of soil particles. Tellus 40B, 494–503.

Lee, B.K., Jun, N.Y., Lee, H.K., 2004. Comparison of particulate matter characteristics before, during, and after Asian dust events in Incheon and Ulsan, Korea. Atmospheric Environment 38, 1535–1545.

Lee, C.T., Chuang, M.T., Chan, C.C., Cheng, T.J., Huang, S.L., 2006. Aerosol characteristics from the Taiwan aerosol supersite in the Asian yellow-dust periods of 2002. Atmospheric Environment 40, 3409–3418.

Ma, C.J., Kasahara, M., Holler, R., Kamiya, T., 2001. Characteristics of single particles sampled in Japan during the Asian dust-storm period. Atmospheric Environment 35, 2707–2714.

Mamane, Y., Gottlieb, J., 1989. Heterogeneous reactions on minerals with sulfur and nitrogen oxides. Journal of Aerosol Science 20, 303–311.

Mamane, Y., Gottlieb, J., 1992. Nitrate formation on sea-salt and mineral particles—a single particle approach. Atmospheric Environment 26A, 1763–1769.

Mori, I., Nishikawa, M., Tanimura, T., Quan, H., 2003. Change in size distribution and chemical composition of kosa (Asian dust) aerosol during long-range transport. Atmospheric Environment 37, 4253–4263.

Park, M.H., Kim, Y.P., Kang, C.H., 2003. Aerosol composition change due to dust storm: measurements between 1992 and 1999 at Gosan, Korea. Water, Air, and Soil Pollution: Focus 3, 117–128.

Park, S.S., Kim, Y.J., 2004. $PM_{2.5}$ particles and size-segregated ionic species measured during fall season in three urban sites in Korea. Atmospheric Environment 38, 1459–1471.

Song, H.C., Carmichael, G.R., 2001. A three-dimensional modeling investigation of the evolution processes of dust and sea-salt particles in East Asia. Journal of Geophysical Research 106, 18131–18154.

Sun, Y., Zhuang, G., Wang, Y., Han, L., Dan, M., Guo, J., Zhang, W., Wang, Z., Hao, Z., 2004. The air-borne particulate pollution in Beijing—concentration, composition, distribution and sources. Atmospheric Environment 38, 5991–6004.

Taylor, S.R., 1964. Abundance of chemical elements in the continental crust: a new table. Geochimica et Cosmochimica Acta 28, 1273–1285.

Trochkine, D., Iwasaka, Y., Matsuki, A., Yamada, M., Kim, Y.S., Zhang, D., Shi, G.Y., Shen, Z., Li, G., 2003. Comparison of the chemical composition of mineral particles collected in Dunhuang, China and those collected in the free troposphere over Japan: possible chemical modification during long-range transport. Water, Air, and Soil Pollution: Focus 3, 161–172.

Usher, C.R., Michel, A.E., Grassian, .H., 2003. Reactions on mineral dust. Chemical Review 103, 4883–4939.

Wang, Y., Zhuang, G., Tang, A., Yuan, H., Sun, Y., Chen, Sh., Zheng, A., 2005a. The ion chemistry and the source of $PM_{2.5}$ aerosol in Beijing. Atmospheric Environment 39 (21), 3771–3784.

Wang, Y., Zhuang, G., Sun, Y., An, Zh., 2005b. Water-soluble part of the aerosol in the dust storm season—evidence of the mixing between mineral and pollution aerosols. Atmospheric Environment 39, 7020–7029.

Wang, Z., Akimoto, H., Uno, I., 2002. Neutralization of soil aerosol and its impact on the distribution of acid rain over East Asia: observations and model results. Journal of Geophysical Research 107 (D19), 4389.

Yong-Seung, C., Hak-Sung, K., Kie-Hyon, P., Jugder, D., Tao, G., 2005. Observations of dust-storms in China, Mongolia and associated dust falls in Korea in spring 2003. Water, Air and Soil Pollution: Focus 5, 15–35.

Yuan, H., Wang, Y., Zhuang, G., 2003. Simultaneous determination of organic acids, methanesulfonic acid and inorganic anions in aerosol and precipitation samples by ion chromatography. Journal of Instrumental Analysis 22, 11–14 (in Chinese).

Zhang, D., Iwasaka, Y., 2001. Chlorine deposition on dust particles in marine atmosphere. Geophysical Research Letters 28, 3613–3616.

Zhang, D., Zang, J., Shi, G., Iwasaka, Y., Matsuki, A., Trochkin, D., 2003. Mixture state of individual Asian dust particles at a coastal site of Qingdao, China. Atmospheric Environment 37, 3895–3901.

Zhang, Y., Sunwoo, Y., Kothamarthi, V., Carmichael, G.R., 1994. Photochemicaloxidant processes in the presence of dust: an evaluation of the impact of dust on particulate nitrate and ozone formation. Journal of Applied Meteorology 33, 813–824.

Zhou, M., Okada, K., Qian, F., Wu, P.-M., Su, L., Casareto, B.E., Shimohara, T., 1996. Characteristics of dust storm particles and their long-range transport from China to Japan—case studies in April 1993. Atmospheric Research 40, 19–31.

Zhuang, G., Yi, Z., Duce, R.A., Brown, P.R., 1992. Link between iron and sulfur suggested by the detection of Fe(II) in remote marine aerosols. Nature 355, 537–539.

Zhuang, G., Guo, J., Yuan, H., Zhao, C., 2001. The compositions, sources, and size distribution of the dust storm from China in spring of 2000 and its impact on the global environment. China Science Bulletin 46, 895–901.